



## Diffusion and viscous flow in bulk glass forming alloys

A. Bartsch<sup>a</sup>, V. Zöllmer<sup>a</sup>, K. Rätzke<sup>a</sup>, A. Meyer<sup>b</sup>, F. Faupel<sup>a,\*</sup>

<sup>a</sup> Institut für Materialwissenschaft – Materialverbunde, Technische Fakultät, Christian-Albrechts Universität zu Kiel, Kaiserstr. 2, 24143 Kiel, Germany

<sup>b</sup> Institut für Materialphysik im Weltraum, Deutsches Zentrum für Luft- und Raumfahrt (DLR), 51170 Köln, Germany

### ARTICLE INFO

#### Article history:

Received 19 September 2010

Received in revised form 1 November 2010

Accepted 17 November 2010

Available online 25 November 2010

#### Keywords:

Diffusion

Viscosity

Stokes–Einstein equation

Mode-coupling theory

Isotope effect

Radiotracer technique

Quasi-elastic neutron scattering

### ABSTRACT

We review radiotracer diffusion and isotope measurements in bulk glass forming alloys from the glassy state to the equilibrium melt and compare diffusion and viscous flow. In the glassy as well as in the deeply supercooled state below the critical temperature  $T_c$ , where the mode coupling theory predicts a freezing-in of liquid-like motion, very small isotope effects indicate a highly collective hopping mechanism. Not only in the glassy state but also in the supercooled state below  $T_c$  the temperature dependence of diffusion is Arrhenius-like with an effective activation enthalpy. A clear decoupling takes place between the diffusivities of the individual components of the alloys and between time scales related to diffusive transport and viscous flow. While the component decoupling is small for the smaller components a vast decoupling of more than 4 orders of magnitude is observed in Pd–Cu–Ni–P alloys between the diffusivity of the large majority component Pd and of the smaller components at the glass transition temperature  $T_g$ . The diffusivities of all components merge close to the critical temperature  $T_c$  of mode coupling theory. Above  $T_c$ , the onset of liquid-like motion is directly evidenced by a gradual drop of the effective activation energy. This strongly supports the mode coupling scenario. The isotope effect measurements show atomic transport up to the equilibrium melt to be far away from the regime of uncorrelated binary collisions. For Pd, in contrast to the behavior of single component molecular glass formers, the Stokes–Einstein equation even holds in the entire temperature range below  $T_c$  over at least 14 orders of magnitude. Apparently, the majority component Pd forms a slow subsystem in which the other elements move fast. Rearrangement of the Pd atoms thus determines the viscous flow behavior. The decoupling of atomic mobility seems to arise from a complex interplay between chemical short order and atomic size effects that gets more pronounced on approaching the glass transition temperature. The ability of the bulk glass forming alloys to form a slow subsystem in the liquid state appears to be a key to the understanding of their excellent glass forming properties.

© 2010 Elsevier B.V. All rights reserved.

### 1. Introduction

Even though metallic glasses, also termed amorphous alloys, were first discovered 50 years ago they are currently among the most actively studied metallic materials with many novel, applicable properties [1–3]. Metallic glass forming alloys have also been the focus of research advancing our understanding of liquids and glasses in general [4,5].

The first metallic glasses, in order to prevent crystallization, were prepared by rapidly quenching (106 K/s) a melt of binary or ternary metal–metalloid or of early-late-transition metal alloys, resulting in very thin ( $d \approx 50 \mu\text{m}$ ) ribbons. Since then, continuous alloy developments [6,7] allow low cooling rates now exceeding 1 K/min and hence bulk samples with the smallest dimension of several cm can be prepared. Thus, deeply undercooled metallic

melts are now accessible on experimental time scales, which make possible investigations around and above the caloric glass transition, where previous alloys immediately crystallized.

Since metallic glasses are metastable systems there exists a driving force to the crystalline equilibrium state. During the first heat treatment near the glass transition structural relaxation occurs [8–10]. Subsequently, the glass transition sets in, and finally the sample crystallizes. All these processes are mainly governed by diffusion. Diffusion and viscous flow are also crucial in melt processing as well as from the fundamental point of view, particularly with respect to the glass transition.

While for crystalline metals self-diffusion occurs via single jumps involving thermal vacancies [11], the situation for metallic glasses is much more complex. Early experiments were often interpreted in terms of a conventional, vacancy-like mechanism (for reviews see, e.g. [12,13]). Now, there is ample evidence from radiotracer experiments [14–16] and molecular dynamics simulations [17,18] that diffusion in the glassy state generally proceeds via highly collective thermally activated jumps involving many

\* Corresponding author. Tel.: +49 431 880 6225; fax: +49 431 880 6229.  
E-mail address: [ff@tf.uni-kiel.de](mailto:ff@tf.uni-kiel.de) (F. Faupel).

atoms [19]. Molecular dynamics simulations suggest a connection between the low-frequency excitations in glasses observed at low temperatures and collective long-range diffusion at elevated temperatures. Only for large atoms, vacancy-like defects seem to play a role [20] and may give rise to an opposite Kirkendall effect [21]. Vacancy-like defects may also enhance diffusion in as quenched metallic glasses prior to structural relaxation [9] although this effect is not seen in all systems [10]. Diffusion in the glassy state of metallic glass formers has recently been reviewed [19]. Here we will focus on diffusion and viscous flow above the caloric glass transition.

As mentioned above, for the so-called bulk glass forming alloys, the undercooled melt above the caloric glass transition temperature becomes accessible. This allows testing of recent theories of the glass transition and the dynamics of undercooled systems. Among these the most advanced theory describing the slowing down of liquid-like motion is the mode coupling theory (MCT) [22,23]. In this extension of the hydrodynamic theory of fluids a kinetic freezing of microscopic (liquid-like) viscous flow is predicted at a critical temperature  $T_c$  far above the caloric glass transition temperature  $T_g$ . Below this critical temperature only thermally activated hopping processes should be possible and are envisioned as highly collective medium assisted hopping in an augmented version of the mode coupling theory which includes the behavior below  $T_c$  [22,23].

Bulk glass forming alloys, for the first time in metallic systems, allow diffusion experiments to be carried out from the glassy state up to the equilibrium melt. In conventional metallic melts, due to their low viscosity, diffusion experiments are normally affected by convection [24].

In simple liquids and melts, where diffusion and viscous flow take place by uncorrelated binary collisions, the Stokes–Einstein equation

$$D(T) = \frac{kT}{6\pi r\eta(T)} \quad (1)$$

generally holds. Here,  $D$  and  $\eta$  are diffusivity and viscosity, respectively,  $k$  is the Boltzmann constant,  $T$  the absolute temperature and  $r$  is the radius of the diffusing species [12]. In the supercooled state of metallic glass forming alloys a break down of the Stokes–Einstein equation has already been reported by Geyer et al. [25]. Recent molecular dynamics simulations on a binary Lennard–Jones mixture have shown the breakdown of the Stokes–Einstein relation at a temperature between the melting temperature and the critical temperature  $T_c$  [26]. The breakdown of the Stokes–Einstein relation was also observed in single component glass formers [27]. Now, most explanations are centered around the concept of dynamical heterogeneity, i.e. the existence of spatially correlated regions of relatively high or low mobility that persist for finite lifetime in the supercooled liquid, and that grow in size as the temperature decreases [28,29].

In the present review we report on our recent results of radiotracer diffusion experiments in bulk glass forming Pd-alloys from the glassy state to the equilibrium melt and compare them with viscosity data from the literature [30–32]. For the first time, a complete set of data for all components is available over the whole relevant temperature range. Special attention is devoted to the change in atomic dynamics around  $T_c$  where the decoupling behavior is now accessible for the individual components. In addition, a comparison of the equilibrium melt with the dynamics of simple liquids will be made.

## 2. Experimental methods

The glasses were prepared as published in, e.g. [33]. The caloric glass transition temperatures were determined by means of differential scanning calorimetry (DSC) at a heating rate of

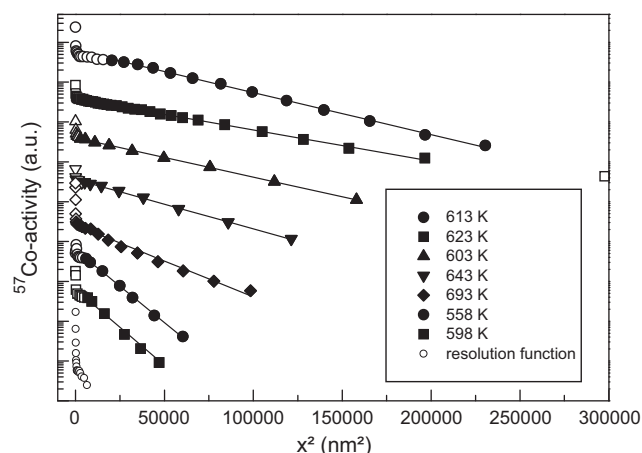


**Fig. 1.**  $^{57}\text{Co}$ -penetration profiles in the glass forming alloy  $\text{Pd}_{40}\text{Cu}_{30}\text{Ni}_{10}\text{P}_{20}$  at temperatures as given. Profiles were shifted on the  $y$ -axis for better comparison. Open symbols are affected by surface artifacts and were not taken into account in the evaluation. The resolution function of the microsectioning technique is shown, too (from [39]).

20 K/min to 577 K. All samples were checked by X-ray diffraction for crystallinity before and after thermal treatment. Diffusion experiments were performed with the well established radiotracer technique, as described in, e.g. [34,35]. Tracers were either commercially available ( $^{32}\text{P}$ ,  $^{57}\text{Co}$ ,  $^{60}\text{Co}$ ) or produced by irradiation of a suitable non-radioactive isotope in the research reactor of the Hahn–Meitner Institute in Berlin ( $^{103}\text{Pd}$ ). After cutting the samples (diameter 10 mm, thickness 1 mm) and polishing the samples the tracer elements were flash-evaporated onto the sputter-cleaned surfaces. The samples were annealed on a heated copper plate or in specially designed graphite crucibles for temperatures and times deduced from the TTT diagram [36,37].

The serial sectioning has been performed either by the sputtering technique, employing an Ar-ion beam similar to the one described in [34] or for larger penetration depths, serial sectioning was performed by mechanical grinding using emery paper of different grain sizes. After serial sectioning the tracer concentration of the respective tracer was determined in each section by use of an intrinsic Ge-detector ( $^{57}\text{Co}$ ,  $^{60}\text{Co}$ , and  $^{103}\text{Pd}$ ). In the case of  $^{32}\text{P}$ , a suitable method for the detection of the  $\beta$ -decay with the liquid scintillation counter taking into account the simultaneous usage of  $^{57}\text{Co}$  had to be established.

The diffusivity was obtained from the thin film solution of Fick's second law.

$$c(x, t) = \frac{I_0}{\sqrt{\pi Dt}} \cdot \exp\left(\frac{-x^2}{4Dt}\right) \quad (2)$$

Here,  $D$  denotes the diffusivity,  $t$  is the annealing time,  $x$  is the penetration depth and,  $I_0$  is the initial layer thickness. Typical penetration profiles are shown in Figs. 1 and 2(a). Only closed symbols represent long-range diffusion and were taken into account for the determination of the diffusivities whereas data points shown as open symbols are affected by surface hold-up or sputtering artifacts, respectively. These effects are well-known from earlier work [39]. The resolution function of the sputtering technique is also shown in Figs. 1 and 2(a). To obtain this function, serial sectioning was performed on a non-annealed sample. The tail at large penetration depths originates from tracer atoms that were first distributed onto components other than the collector foil and then sputtered off again. The resolution function shows that effects on the evaluation of diffusivities and isotope effects are negligible within experimental errors.

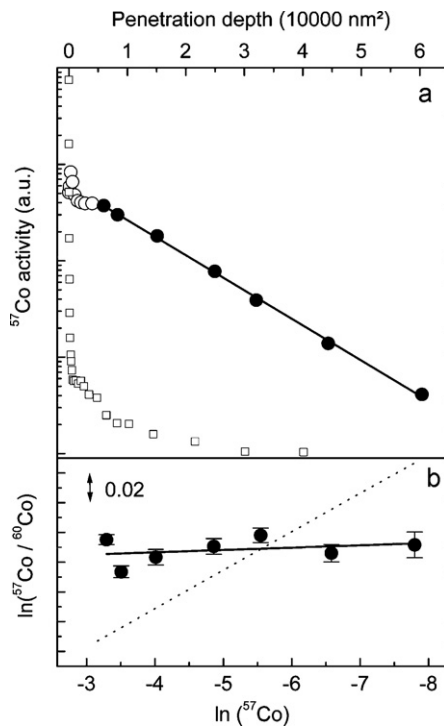


**Fig. 2.** (a) Typical penetration profile of Co diffusion in Pd<sub>40</sub>Cu<sub>30</sub>Ni<sub>10</sub>P<sub>20</sub> at 603K, annealed for 1 h (above). The activity is plotted vs. the square of penetration depth. The resolution function of the sputtering technique is shown, too (open squares). (b) A typical isotope effect profile of Co diffusion in Pd<sub>40</sub>Cu<sub>30</sub>Ni<sub>10</sub>P<sub>20</sub> is shown below. The activity ratio of <sup>57</sup>Co and <sup>60</sup>Co is plotted vs. the <sup>57</sup>Co activity on a logarithmic scale. The dotted line yields an isotope effect of  $E = 1$  and is shown for comparison.

The diffusivities were calculated from the slopes  $m = -1/(4Dt)$  of the straight lines fitted to the data according to Eq. (2). The experimental errors in the absolute diffusivity are about 20% and are smaller than symbol size in the following figures. The major contributions originate from uncertainties in the depth and temperature measurements [10,39].

The isotope effect  $E$  is defined as:

$$E = \frac{D_\alpha/D_\beta - 1}{\sqrt{m_\beta/m_\alpha} - 1} \quad (3)$$

$E$  is defined thus that  $E=1$  for an ideal single jump diffusion mechanism with exhibits a  $1/m^{1/2}$  mass dependence arising from the attempt frequency.

It can be calculated from the following equation

$$\ln \left[ \frac{c_\alpha(x, t)}{c_\beta(x, t)} \right] = \text{const.} - \left[ \frac{D_\alpha/D_\beta - 1}{\ln c_\alpha(x, t)} \right] \quad (4)$$

which results from simple rearrangement of the thin-film solution for the two isotopes.

A typical result is shown in Fig. 2(b). One notes that the isotope effect in the present Pd-based alloy in the supercooled liquid state is close to zero, much smaller than the value of unity, expected for an ideal single jump process.

The (almost) vanishing isotope effects were also observed in the glassy state of conventional metallic glasses [10,14,16]. They were interpreted as a result of the strong dilution of the ordinary  $m^{-1/2}$  mass dependence of the attempt frequency by coordinated hopping of a large number of atoms. This view is consistent with the results from molecular dynamics simulations, where mainly chain-like displacements were observed [42].

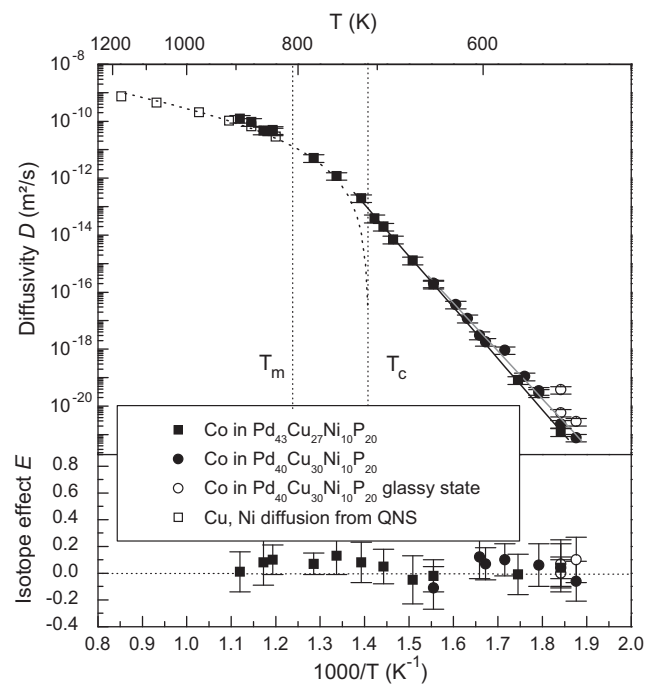


**Fig. 3.** (a) Temperature and (b) mass dependence (isotope effect) of Co-diffusion in Pd<sub>40</sub>Cu<sub>30</sub>Ni<sub>10</sub>P<sub>20</sub> and Pd<sub>43</sub>Cu<sub>27</sub>Ni<sub>10</sub>P<sub>20</sub>. The temperature dependence is plotted as  $\ln D$  vs.  $1/T$  (Arrhenius plot) together with diffusion data from quasielastic neutron scattering (QNS) (open squares [33], for a detailed discussion of these data see text). The open circles refer to the glassy state, the solid symbols refer to the supercooled liquid state and the equilibrium liquid state, respectively. The quasi-eutectic melting temperature  $T_m$  is displayed.

### 3. Diffusion in Pd based alloys

Fig. 3 shows the diffusivities of Co and the corresponding isotope effects in Pd<sub>40</sub>Cu<sub>30</sub>Ni<sub>10</sub>P<sub>20</sub> and Pd<sub>43</sub>Cu<sub>27</sub>Ni<sub>10</sub>P<sub>20</sub> alloys. The upper part displays the Arrhenius plot for Co-diffusion in the two Pd–Cu–Ni–P alloys [35,38,43]. Here, filled symbols correspond to the well-relaxed supercooled liquid state. The temperature dependence follows an Arrhenius-like behavior. This is in accordance with the aforementioned linear Arrhenius plots reported for other bulk glass forming alloys in the deeply supercooled melt. One must point out that the Arrhenius parameters have to be regarded as effective quantities due to the structural changes occurring in the metastable equilibrium state with increasing temperature.

Open symbols, seen at lower temperatures represent samples that were annealed for relatively short times not allowing relaxation into the supercooled equilibrium state. Here the diffusivity is much higher (note the logarithmic scale) indicating an enhancement caused by incomplete relaxation to the supercooled liquid state. Therefore, these data points can be attributed to the non-equilibrium glassy state [44]. The drop of the diffusivity is mainly related to the annealing of excess volume during relaxation.

We were able to measure the isotope effect  $E$  in the glassy and in the supercooled liquid state [38] during isothermal structural relaxation. The isotope effect data are displayed in Fig. 3 together with the diffusivities. Though the diffusivity decreases by an order of magnitude during relaxation from the glassy to the supercooled liquid state at 543 K, there is no change in isotope effect. The isotope effect is very small in the whole supercooled liquid range as well as in the glassy state. This lends strong support to the view [19,38,40,43] that the diffusion mechanism does not change at the caloric glass transition and that diffusion occurs by highly collective hopping in the glassy and in the supercooled liquid state well below  $T_c$ . In particular, we can rule out a change in the diffusion

mechanism at  $T_g$  from single atom hopping (below  $T_g$ ) to predominantly collective diffusion as proposed in the literature for Be in Vitreloy 4 [45–47]. The absence of a change of the diffusion mechanism at  $T_g$  corroborates results from computer simulations [48,49] and is in agreement with the mode coupling theory, which predicts a freezing in of liquid-like motion at  $T_c$  well above  $T_g$  [50,51]. As mentioned above, below  $T_c$ , the augmented mode coupling theory [22,23] envisions diffusion as medium assisted highly collective hopping. Apparently, diffusion between  $T_c$  and  $T_g$  proceeds by solid-like hopping (although highly collective) despite the fact that macroscopically the samples are in the (highly viscous) molten, i.e. liquid state. A clear signature of highly collective hopping was also seen in our earlier isotope effect measurements in the supercooled liquid state of Zr-based systems [40].

As shown in Fig. 3, the diffusion and isotope effect data obtained in one of the most stable metallic glass-forming alloys  $\text{Pd}_{43}\text{Cu}_{27}\text{Ni}_{10}\text{P}_{20}$  below  $T_c$  are in full accordance with the data for  $\text{Pd}_{40}\text{Cu}_{30}\text{Ni}_{10}\text{P}_{20}$  and also encompass the range above  $T_c$  up to the equilibrium melt. Below  $T = 700$  K one notes Arrhenius type behavior. Although there are minor differences in the absolute values of the diffusivities in these two alloys, the values of the Arrhenius plot, particularly in the overlapping temperature range, demonstrate that the general tendency in the two alloys is the same.

Moreover, in the equilibrium melt one notes that the diffusivities determined from quasi-elastic neutron scattering experiments, reflecting mainly the Cu and Ni diffusivities [33], agree very well with the Co-diffusivities from the present work. Since measurements of diffusivities from neutron scattering are not prone to convection, the excellent agreement with our radiotracer data shows that the latter are not affected by convection. This is in contrast to many previous experiments in metallic melts with lower viscosity [24]. We note that our results are in full accord with  $\mu\text{g}$  experiments performed by Griesche and coworkers during FOTON mission [52,53].

The neutron scattering experiments also allowed monitoring of the fast  $\beta$ -relaxation. From these data the critical temperature  $T_c$  (see Fig. 3) and the exponent  $\gamma$  of the mode coupling theory were determined [33]. Knowing  $T_c$ , one can directly test predictions of the mode coupling theory. In particular, our data shown in Fig. 3 clearly provide evidence of a change in the atomic dynamics at  $T_c$ . Here the effective activation energy  $-k \partial \ln D / \partial T^{-1}$  (slope in Fig. 3) starts to drop gradually as expected from the onset of liquid-like motion in the mode coupling scenario. Due to the increasing influence of liquid-like motion the nearest neighbor barriers should gradually decrease as the temperature is increased above  $T_c$ . As mentioned earlier, above  $T_m$  in the equilibrium melt, our Co diffusivities are within the statistical error equal to the diffusivities derived from inelastic neutron scattering [33]. We note that at  $T_m$  the diffusivities are 2 orders of magnitude smaller than that of ordinary liquids [54].

Above  $T_c$  the idealized mode coupling theory (that neglects mass transport via hopping below  $T_c$ ) predicts

$$\frac{1}{D} \propto \left[ \frac{(T - T_c)}{T_c} \right]^\gamma \quad (5)$$

The dashed line in Fig. 3 represents Eq. (5) using the  $T_c = 710$  K and the exponent  $\gamma = 2.7$  from the analysis of the localized cage motion as measured by inelastic neutron scattering [33]. Our diffusion data are even in quantitative agreement with the MCT predictions. The singularity at  $T_c$  is not expected in real systems, and the augmented MCT that takes into account hopping processes [22,23] predicts a smooth transition to Arrhenius behavior in the way reflected in our data (Fig. 3).

It has to be pointed out that other theories, including the free volume theory first introduced by Cohen and Turnbull, which already involves the cage effect, also predict a change in the slope

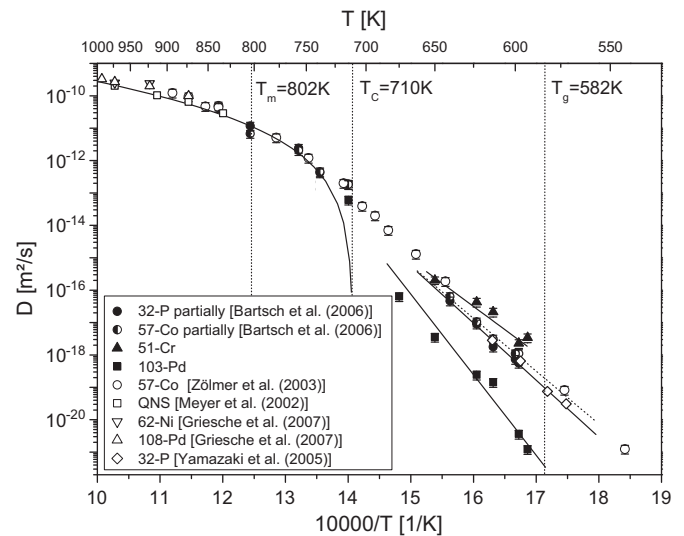


**Fig. 4.** Diffusivities of  $^{32}\text{P}$ ,  $^{57}\text{Co}$ ,  $^{51}\text{Cr}$  and  $^{103}\text{Pd}$  in  $\text{Pd}_{43}\text{Cu}_{27}\text{Ni}_{10}\text{P}_{20}$  in an Arrhenius representation. The dashed lines represent melting temperature  $T_m$ , critical temperature  $T_c$  of mode coupling theory and calorimetric glass transition temperature  $T_g$  (DSC, 20 K/min).  $^{32}\text{P}$ - and  $^{57}\text{Co}$ -data (full and half-filled circles) for  $T < 650$  K are from [57].  $^{57}\text{Co}$ -data, shown as open circles, are from [35].

of the Arrhenius plot in the supercooled liquid state (for reviews see Refs. [54,55]). However, our observation that liquid-like motion sets in exactly above the critical temperature  $T_c$  of MCT is striking.

In the present alloys the viscosity is still two orders of magnitude higher at the melting point compared to simple metallic melts, and the isotope is very low in the equilibrium melt ( $E \approx 0.05$ ). Below  $T_c$  and in the glassy state such low values have already been discussed above and were attributed to highly collective thermally activated hopping processes. The low  $E$ -values in the equilibrium melt, however, show that the present Pd–Cu–Ni–P melt is still far away from the hydrodynamic regime of uncorrelated binary collisions. This is in strong contrast to simple melts such as liquid Sn, which shows a rather large isotope effect [56]. In the absence of significant correlation, the isotope effect should be of the order of unity in simple liquids [53]. Molecular dynamics simulations indicate a relationship between isotope effect and density of the liquid. This suggests the present very low  $E$ -values to be due to the small density difference between glassy and liquid state of only about 3% [49]. The strongly coordinated atomic motion evidenced by the low isotope effect value in the equilibrium liquid appears to be crucial to the excellent glass forming ability.

Very recently, we measured the tracer diffusivities of various elements in  $\text{Pd}_{43}\text{Cu}_{27}\text{Ni}_{10}\text{P}_{20}$  to investigate the decoupling behavior [41]. The results are shown together with some data from the literature in Fig. 4. Comparing the  $^{57}\text{Co}$  diffusivities of this work in the undercooled melt to the ones previously measured in our laboratory (also depicted in Fig. 4), one can see a small difference [35,43]. Both series of measurements were done in a similar way but with different  $\text{Pd}_{43}\text{Cu}_{27}\text{Ni}_{10}\text{P}_{20}$  batches. Both batches were checked with DSC as well as EDX, and no differences were found within the high accuracy of the methods used. We assume that even very small differences in the composition of the alloy in the steep multidimensional eutectic valley can have a noticeable influence on diffusivities (this could also explain some discrepancies in the literature, see below). We remark that the  $^{57}\text{Co}$  diffusivity is rather similar to the Ni diffusivity as shown earlier [19 and references therein]. We note, however, that the present difference of a factor of two is quite small in comparison to the orders of magnitude effects concomitant with the investigated decoupling behavior.

As seen in Fig. 4, decoupling of the diffusivities sets in somewhat above  $T_c$  and reaches several orders of magnitude between the fastest and slowest component near  $T_g$ . Decoupling is a signature of solid-like hopping over barriers, which – unlike in crystals – is envisioned as a highly collective process. The barriers are expected to freeze in at  $T_c$  and to decay quickly somewhat above  $T_c$ , which is as much as 128 K above the caloric glass transitions temperature  $T_g$  (at 20 K/min) in the present metallic glass former. We note that the slowest element is not phosphorous but the majority component palladium in contrast to expectations stated in the literature where phosphorous was discussed as a covalent network former [58].

Our  $^{32}\text{P}$  diffusion coefficients agree well  $^{32}\text{P}$  diffusion coefficients measured by Yamazaki in a similar alloy [58]. These authors also measured one diffusion coefficient for Cu in their alloy and found it nearly two orders of magnitude higher than the corresponding phosphorous diffusivity and similar to  $^{63}\text{Ni}$  diffusivities from Nakajima et al. in another Pd–Cu–Ni–P alloy [59]. Yamazaki et al. concluded that this large difference between their phosphorous diffusivity on the one hand, and the Cu and Ni diffusivities on the other hand, is indicative of the strongly covalent bond character of phosphorus in the present alloy. However, comparing our  $^{57}\text{Co}$  diffusivities with those of  $^{63}\text{Ni}$  measured by Nakajima et al. in a Pd<sub>40</sub>Cu<sub>30</sub>Ni<sub>10</sub>P<sub>20</sub> alloy one can see again a large difference by two orders of magnitude. Since neither the time dependence of the diffusivities nor all of the diffusion profiles were reported by Nakajima et al., it is difficult to assess the origin of the differences. One possible explanation could be differences in the sample preparation resulting in different alloy compositions. As discussed above, even relatively small differences in composition may cause large differences in the diffusivities.

The crucial role of Pd is also reflected in the fact that a vast decoupling of more than 4 orders of magnitude is observed between the diffusivity of Pd and of the smaller components, at the glass transition temperature  $T_g$  whereas little decoupling is seen among the small components. We point out that this decoupling of the diffusivities of the individual components (component decoupling) has to be clearly discriminated from viscous decoupling, i.e. the decoupling of diffusion and viscous flow discussed in the following section. The viscous decoupling could be regarded as just a consequence of the effect of the broadening of the distribution of mobilities and the different ways transport and relaxation sample that distribution, i.e. viscous decoupling (because it involves two qualitatively different physical quantities) may be considered as reflecting something rather general about the statistics of dynamics. In contrast, the component decoupling must have an explicit structural origin and reveals information on the relation between composition and atomic dynamics.

#### 4. Comparison of diffusion and viscous flow in Pd based alloys

In addition to the decoupling behavior of the diffusivities, an important characteristic of the atomic dynamics is the relationship between diffusion and viscous flow. Fortunately, for the glass forming alloy Pd<sub>43</sub>Cu<sub>27</sub>Ni<sub>10</sub>P<sub>20</sub> viscosity data are available from Refs. [30,31]. In particular, it has to be noted that the viscosities are not significantly dependent on concentration, indicating that chemical effects are of minor importance and packing fraction plays a major role [60]. These viscosities are plotted in Fig. 5 together with viscosities calculated from the individual diffusivities in Fig. 4 from the Stokes–Einstein (SE) equation (Eq. (1)) [41]. One sees that the Stokes–Einstein equation holds perfectly in the equilibrium melt and down to near  $T_c$  where it starts to break down. The disparity reaches 4 orders of magnitude in the supercooled liquid state near the caloric glass transition. A striking observation, however,

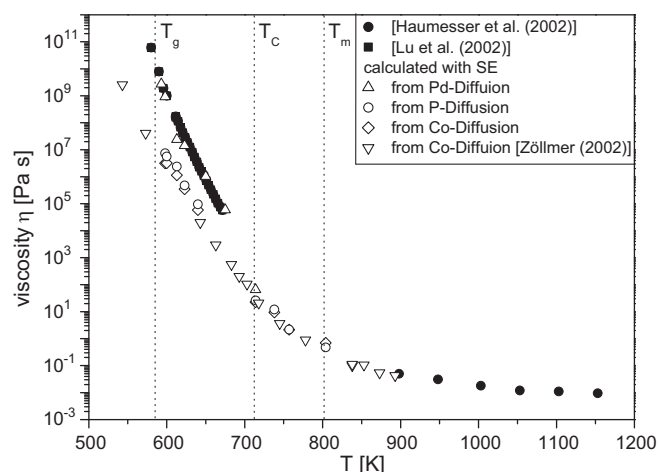


**Fig. 5.** Comparison of diffu-viscosity and measured viscosity in Pd<sub>43</sub>Cu<sub>27</sub>Ni<sub>10</sub>P<sub>20</sub>. Filled black symbols show measured viscosity from Haumesser et al. [31], and Lu et al. [30]. All other symbols show diffu-viscosities, calculated via Stokes Einstein from measured diffusivities. Additionally, we included with dashed lines melting temperature  $T_m$ , critical temperature  $T_c$  from Mode Coupling Theory and caloric glass transition temperature  $T_g$  (DSC, 20 K/min).

is that despite this strong decoupling (see also Fig. 4) the SE equation holds rigorously for the majority component palladium which also has the largest atomic size. Apparently, Pd forms a slow subsystem in the supercooled melt inside which the smaller elements carry out fast diffusion. This is even more surprising because Pd is not expected to form a covalent network in this metallic system. Obviously, viscous flow requires the subsystem to break up because rearrangement of the Pd atoms and viscous flow occur on the same time scale according to our results.

The present observation of the validity of the SE equation for Pd over at least 14 orders of magnitude is also striking in view of its aforementioned recently observed breakdown in a single component molecular glass formers [29] and the fact that the break down of the SE equation is now generally attributed to dynamic heterogeneity [28,29]. Even though our observation does not challenge this explanation it appears to be quite unexpected and rises interesting new questions with respect to the bonding characteristics in the bulk glass forming alloys and on the origin of the formation of slow subsystems [61]. In this connection we note that Kumar et al. [62] in their molecular dynamics simulations of hard sphere fluids with size disparity also found remaining ‘sedentary’ particles which formed a slow subsystem and were unaware of the breakdown of the SE equation. This also shows that the formation of slow subsystems does not require covalent bonding similar to oxide glasses. Concerning the contrasting behavior to the single component molecular glass formers, their glass forming ability is not due to dynamic asymmetry caused by size disparity or chemical short range order but results from a complex and highly asymmetric structure. In systems with dynamic asymmetry like multicomponent metallic glass formers, the building up of a slow subsystem appears to be the crucial factor in glass formation.

#### Acknowledgements

The authors thank H. Teichler (Georg-August University at Göttingen) and Thomas Voigtmann (DLR Köln) for fruitful discussions and acknowledge financial support by German Science Foundation (DFG) under the projects Ra 796/3, Ra 796/4 and Me 1958/2. We would like to thank the HMI Berlin for irradiation of Pd tracers.

## References

- [1] A.L. Greer, *Mater. Today* 12 (2009) 14.
- [2] A. Inoue, N. Nishiyama, *MRS Bull.* 32 (2007) 651.
- [3] A. Inoue, *Mater. Sci. Forum* 691 (1995) 179–181.
- [4] W.H. Wang, C. Dong, C.H. Shek, *Mater. Sci. Eng. R* 44 (2004) 45.
- [5] A.R. Yavari, J.J. Lewandowski, J. Eckert, *MRS Bull.* 32 (2007) 635.
- [6] A. Peker, W.L. Johnson, *Appl. Phys. Lett.* 63 (1993) 2342.
- [7] T. Zhang, A. Inoue, T. Masumoto, *Mater. Trans. Jpn. Inst. Metal* 32 (1991) 1005.
- [8] W. Ulfert, J. Horvath, W. Frank, H. Mehrer, *Cryst. Latt. Def. Am. Mater.* 18 (1999) 519.
- [9] K. Rätzke, P.W. Hüppe, F. Faupel, *Phys. Rev. Lett.* 68 (1992) 2347.
- [10] A. Heesemann, K. Rätzke, V. Zöllmer, F. Faupel, *New J. Phys.* 3 (2001), 6.1.
- [11] Paul G. Shewmon, *Diffusion in Solids, Minerals, Metals & Materials Society, Warrendale, PA, 1989.*
- [12] F. Faupel, *Phys. Status Solidi (a)* 134 (1992) 9.
- [13] W. Frank, J. Horvath, H. Kronmüller, *Mater. Sci. Eng.* 97 (1988) 415.
- [14] F. Faupel, P.W. Hüppe, K. Rätzke, *Phys. Rev. Lett.* 65 (1990) 1219.
- [15] P. Klugkist, K. Rätzke, S. Rehders, P. Troche, F. Faupel, *Phys. Rev. Lett.* 80 (1998) 3288.
- [16] A. Heesemann, V. Zöllmer, K. Rätzke, F. Faupel, *Phys. Rev. Lett.* 84 (2000) 1467.
- [17] H. Teichler, *Def. Diff. Forum* 143–147 (1997) 717.
- [18] C. Oligschleger, H.R. Schober, *Phys. Rev. B* 59 (1999) 811.
- [19] F. Faupel, W. Frank, M.-P. Macht, H. Mehrer, V. Naundorf, K. Rätzke, H.R. Schober, S.K. Sharma, H. Teichler, *Rev. Mod. Phys.* 75 (2003) 237.
- [20] P. Klugkist, K. Rätzke, F. Faupel, *Phys. Rev. Lett.* 81 (1998) 614.
- [21] K.N. Tu, T.C. Chou, *Phys. Rev. Lett.* 61 (1988) 1862.
- [22] W. Götze, L. Sjögren, *J. Non-Cryst. Solids* 131–133 (1991), 153 and 161.
- [23] W. Götze, *J. Phys.: Condens. Matter* 11 (1999) A1.
- [24] N.H. Nachtrieb, *Ber. Bunsenges. Phys. Chem.* 80 (1976) 678.
- [25] U. Geyer, W.L. Johnson, S. Schneider, Y. Qiu, T.A. Tombrello, M.-P. Macht, *Appl. Phys. Lett.* 69 (1996) 2492.
- [26] F. Bordat, M. Affouard, F. Descamps, Müller-Plathe, *J. Phys.: Condens. Matter* 15 (2003) 5397.
- [27] S.F. Swallen, P.A. Bonvallet, R.J. McMahon, M.D. Ediger, *Phys. Rev. Lett.* 90 (2003) 015901.
- [28] P. Royall, et al., *Nat. Mater.* 7 (2008) 556.
- [29] S.F. Swallen, K. Traynor, R.J. McMahon, M.D. Ediger, T.E. Mates, *Phys. Rev. Lett.* 102 (2009) 065503.
- [30] I.-R. Lu, G.P. Görlner, H.J. Fecht, R. Willnecker, *J. Non-Cryst. Solids* 312–314 (2002) 547.
- [31] H. Haumesser, J. Bancillon, M. Daniel, J.P. Garandet, J.C. Barbe, N. Kernevez, *Int. J. Thermophys.* 23 (2002) 1217.
- [32] A. Masuhr, T.A. Waniuk, R. Busch, W.L. Johnson, *Phys. Rev. Lett.* 82 (1999) 2290.
- [33] A. Meyer, *Phys. Rev. B* 66 (2002) 134205.
- [34] F. Faupel, P.W. Hüppe, K. Rätzke, R. Willecke, T. Hehenkamp, *J. Vac. Sci. Technol. A* 10 (1992) 92.
- [35] V. Zöllmer, K. Rätzke, F. Faupel, *J. Mater. Res.* 18 (2003) 2688.
- [36] J. Schroers, W.L. Johnson, *Appl. Phys. Lett.* 77 (2000) 1158.
- [37] K. Knorr, M.-P. Macht, H. Mehrer, *MRS Symp. Proc.* 554 (1999) 269.
- [38] V. Zöllmer, K. Rätzke, F. Faupel, A. Rehmet, U. Geyer, *Phys. Rev. B* 65 (2002) 220201(R) (rapid communications).
- [39] H. Ehmler, A. Rehmet, K. Rätzke, F. Faupel, *Def. Diff. Forum* 203–205 (2002) 147.
- [40] H. Ehmler, A. Heesemann, K. Rätzke, F. Faupel, *Phys. Rev. Lett.* 80 (1998) 4919.
- [41] A. Bartsch, K. Rätzke, A. Meyer, F. Faupel, *Phys. Rev. Lett.* 104 (2010) 195901.
- [42] H.R. Schober, C. Gaukel, C. Oligschläger, *Prog. Theor. Phys.* 126 (1997) 67.
- [43] V. Zöllmer, A. Meyer, K. Rätzke, F. Faupel, *Phys. Rev. Lett.* 92 (2003) 195502–195511.
- [44] T. Zumdley, V. Naundorf, M.-P. Macht, G. Froberg, *Ann. Chim.* 27 (2002) 55.
- [45] A.L. Greer, *Nature* 366 (1999) 303.
- [46] X.-P. Tang, U. Geyer, R. Busch, W.L. Johnson, Y. Wu, *Nature* 402 (1999) 160.
- [47] U. Geyer, S. Schneider, W.L. Johnson, Y. Qiu, T.A. Tombrello, M.-P. Macht, *Phys. Rev. Lett.* 75 (1995) 2364.
- [48] H. Teichler, *Phys. Rev. B* 59 (1999) 8473.
- [49] H.R. Schober, *Sol. State Commun.* 119 (2001) 73.
- [50] W. Götze, L. Sjögren, *Rep. Progr. Phys.* 55 (1992) 241.
- [51] W. Götze, L. Sjögren, *Transport. Theory Stat. Phys.* 24 (1995) 801.
- [52] A. Griesche, M.P. Macht, S. Suzuki, K.H. Kraatz, G. Froberg, *Scripta Mater.* 57 (2004) 477.
- [53] S. Suzuki, K.H. Kraatz, A. Griesche, G. Froberg, *Microgravity Sci. XVI FT Technol.* (2005) 127.
- [54] J. Jäckle, *Rep. Progr. Phys.* 49 (1986) 171.
- [55] H.Z. Cummins, G. Li, H.Y. Hwang, G.Q. Shen, W.M. Du, J. Hernandez, N.J. Tao, *Z. Phys. B* 103 (1997) 501.
- [56] G. Froberg, K.-H. Kraatz, H. Wever, *Mater. Sci. Forum* 15–18 (1987) 529.
- [57] A. Bartsch, K. Rätzke, F. Faupel, A. Meyer, *Appl. Phys. Lett.* 89 (2006) 121917.
- [58] Y. Yamazaki, T. Nihei, J. Koike, T. Ohtsuki, *Proc. 1st Int. Conf. Diffusion in Solids and Liquids, 2005*, p. 831.
- [59] H. Nakajima, T. Kojima, T. Zumdley, N. Nishiyama, A. Inoue, *Proc. Int. Conf. Solid–Solid Phase Transformation*, vol. 12, 1999, p. 441.
- [60] S. Mavila Chathoth, A. Meyer, H. Schober, F. Juranyi, *Appl. Phys. Lett.* 85 (2004) 4881.
- [61] G. Biroli, J.P. Bouchaud, *J. Phys.: Condens. Matter* 19 (2007) 205101.
- [62] S.K. Kumar, G. Szamel, J.F. Douglas, *J. Chem. Phys.* 124 (2006) 214501.